



UNIVERSITÀ POLITECNICA DELLE MARCHE
Repository ISTITUZIONALE

Long term correlation and inhomogeneity of the inverted pendulum sway time-series under the intermittent control paradigm

This is the peer reviewed version of the following article:

Original

Long term correlation and inhomogeneity of the inverted pendulum sway time-series under the intermittent control paradigm / Tigrini, A.; Verdini, F.; Fioretti, S.; Mengarelli, A.. - In: COMMUNICATIONS IN NONLINEAR SCIENCE & NUMERICAL SIMULATION. - ISSN 1007-5704. - STAMPA. - 108:(2022).
[10.1016/j.cnsns.2021.106198]

Availability:

This version is available at: 11566/294354 since: 2024-04-25T09:56:25Z

Publisher:

Published

DOI:10.1016/j.cnsns.2021.106198

Terms of use:

The terms and conditions for the reuse of this version of the manuscript are specified in the publishing policy. The use of copyrighted works requires the consent of the rights' holder (author or publisher). Works made available under a Creative Commons license or a Publisher's custom-made license can be used according to the terms and conditions contained therein. See editor's website for further information and terms and conditions.

This item was downloaded from IRIS Università Politecnica delle Marche (<https://iris.univpm.it>). When citing, please refer to the published version.

(Article begins on next page)

Long Term Correlation and Inhomogeneity of the Inverted Pendulum Sway Time-Series under the Intermittent Control Paradigm

Andrea Tigrini^a, Federica Verdini^a, Sandro Fioretti^a, Alessandro Mengarelli^{a,*}

^a*Department of Information Engineering, Università Politecnica delle Marche, 60131, Ancona, Italy*

Abstract

In this study the extended detrended fluctuation analysis (EDFA) was applied to the sway data generated from an inverted pendulum (IP) model, intermittently controlled at the ankle. The time series taken into account was the center of pressure (COP), since it represents the widest used time series in posturography, and it constitutes a natural link between model and data-based analysis approaches for studying the dynamics of the human balance maintenance. COP time-series were obtained by varying the intermittent control parameters (ICP) in a uniform distribution range that ensures IP stability to quantify changes in the long-term correlation and inhomogeneity of the time-series. Globally, EDFA coefficients (α and β) showed to be sensitive to the variations of derivative control gain (D), whereas for proportional gain (P) and ρ parameters no significant trends were observed. However, relations between EDFA coefficients and ρ arose whether derivative gain is examined within a low and high regions of value. For low D gains, both α and β showed a significant correlation with ρ , which disappears when higher D values were considered. Thus EDFA coefficients can provide useful insights about the long-term correlation and local characteristics of COP timeseries, which are strictly related to the control policy adopted

*Fully documented templates are available in the elsarticle package on CTAN.

*Corresponding author

Email addresses: a.tigrini@pm.univpm.it (Andrea Tigrini), f.verdini@staff.univpm.it (Federica Verdini), s.fioretti@staff.univpm.it (Sandro Fioretti), a.mengarelli@pm.univpm.it (Alessandro Mengarelli)

for maintaining balance. This supports the validity of the intermittent motor control paradigm for the human upright stance and suggests the use of EDFA in real posturography applications, in order to extract meaningful information regarding the properties of COP timeseries for different groups of patients.

Keywords: Center of Pressure (COP), Intermittent control, Extended detrended fluctuation analysis (EDFA)

1. Introduction

The study of bipedal upright stance and balance maintenance has fascinated many different scientific disciplines. Indeed, understanding the hidden mechanisms that the central nervous system (CNS) employs to control the body mechanics is fundamental in neurorobotics to embody intelligence in humanoid robots [1, 2], but even in neuroscience and posturography, to better understand how pathologies affecting CNS may impact on the motor control [3, 4]. In this scenario, approaches that combine biomechanical modeling of the stance and the analysis of time-series, such as the evolution of the center of mass (COM) and the center of pressure (COP) [5, 6, 7], grounded the bases for a deeper comprehension of the motor control policies actuated by the CNS.

Although stiffness-based stabilizing mechanisms and continuous control paradigm are widely used in literature to model the neuromuscular control of stance [8, 9], the intermittent control approach demonstrated to be supported by physiological evidence [10]. As first, muscle activity is bursting, and it may be mirrored in the control torques at the human joints [6]. Furthermore, Morasso, Schieppati, and Sanguineti [11, 12] highlighted the inability of the ankle stiffness alone to compensate the whole body gravity pull, without an active mechanism played by the CNS [5]. Moreover, the intermittent control policy can generalize a continuous one, as highlighted in [7]. Thus, despite the real motor control paradigm of the stance maintenance is unknown, it is plausible that the CNS can take advantage from the body structure in order to develop a control strategy that does not act continuously [10]. Indeed, global stability of the system can be

24 obtained switching between unstable dynamics [10, 13], hence through a variable
 25 structure control policy. The idea of intermittency, meant as an agent that acts
 26 when necessary, was hypothesized also by Collins and De Luca [14], following
 27 a time-series analysis approach, i.e. the stabilogram diffusion analysis (SDA)
 28 [14].

29 Despite the two previous perspectives, i.e. model-based and time-series anal-
 30 ysis, are different [7], the need for a unified perspective results of great impor-
 31 tance when one would obtain highly explainable models. Indeed, in [7] the
 32 aforementioned approaches were combined through the approximate bayesian
 33 computation, in order to infer the parameters of the intermittent controller
 34 from posturographic data. This makes more underpinned the interpretation
 35 of the results if compared to models obtained through black box identification
 36 procedures, where high fidelity data fitting could be paid with a limited inter-
 37 pretability. Literature shows other studies that followed the inclusive approach
 38 stated above. In [15] for instance, SDA was applied to simulated COP data
 39 obtained by using a simple inverted pendulum (IP) model, commonly used to
 40 describe the mechanics of the body stance, varying the continuous controller
 41 parameters, and then examining their relation with the SDA coefficients [14].
 42 Also in [10], changes in the intermittent control parameters (ICP) were related
 43 to changes in the power spectral density (PSD) of the sway data. Furthermore,
 44 such PSDs reproduced the multiple law scaling properties observed in data ac-
 45 quired during human quiet stance [10].

46 The investigation of intermittent control models of human stance through
 47 time series analysis approaches is far to be completely assessed. In particular,
 48 as emerged from previous works [15, 16, 6, 17], a possible way to carry on
 49 such investigation is to employ COP model-generated data. This for two main
 50 reasons: firstly, the COP can be directly measured from force platforms without
 51 the need for any motion capture systems, commonly used to estimate the COM.
 52 Thus, the knowledge extracted from the model can be validated through real
 53 data. Secondly, COP is directly related with the control torques generated at
 54 the ankle and upper joints of the body [11, 8, 14], and hence it contains the

sign of the CNS control action. Another important aspect regards the selection of adequate descriptors used to evaluate the COP time-series. In [18] different spatial, temporal and frequency COP descriptors were presented. However, they do not account for the nonlinear properties and long-term correlation of COP data. Instead, other authors approached the study of COP time-series through the use of SDA, rambling and trembling decomposition, sway density curve and detrended fluctuation analysis (DFA) [14, 19, 4, 20, 21]. These are only few of the methodologies employed to capture more detailed information regarding the nature of biological processes behind balance maintenance.

Recently, an extension of the DFA, named extended DFA (EDFA), was proposed in [22]. EDFA grounds its basis on the fact that experimental data often present inhomogeneity due to changes in the dynamics of the systems. This aspect can be encountered in many biological time series, ranging from heart rate to electroencephalography [23, 24]. Moreover, behind EDFA there is the idea to quantify not only the slow variations in the local mean value, as done by DFA, but also to consider other types of non-stationary behaviors, such as those induced by intermittency or faster oscillations [23]. Thus in this study, EDFA was applied to simulated COP time course obtained through intermittent control paradigm, applied to an IP model, and by varying the ICP within a plausible range [10, 7]. Then, EDFA coefficients were computed to assess how changes in the ICP affect posturographic data, and if EDFA can highlight hidden properties of the motor control paradigm employed to stabilize the IP.

The paper is organized as follows. Methods section describes the human stance model based on the intermittent controller used to generate simulated COP, then EDFA principles are recalled. Results are thus presented and discussed in the third section, and concluding remarks reported in the last section end the paper.

82 2. Materials and Methods

83 2.1. Upright stance balance maintenance model and data generation

84 The human balance maintenance model considered in this study was pre-
 85 sented in [10], and it basically develops a variable structure control system to
 86 describe the body sway in quiet conditions. The latter can be modeled through
 87 an IP linearized in the neighborhood of the vertical equilibrium point [10]. Thus,
 88 the dynamics is given by:

$$I\ddot{\theta} = mgh\theta - T \quad (1)$$

89 where θ is the COM sway angle in the sagittal plane, m is the subject body
 90 mass, h is the distance of the COM with respect to the ankle, g is the gravity
 91 acceleration, and I is the moment of inertia of the body around the ankle. The
 92 term $mgh\theta$, hence represents the gravitational toppling torque that is dynam-
 93 ically counterbalanced by T , i.e. the control torque applied at the pendulum
 94 joint. The latter can be modeled as in [10, 6]:

$$T = K\theta + B\dot{\theta} + f_P(\theta_\Delta) + f_D(\dot{\theta}_\Delta) + \sigma\xi \quad (2)$$

95 The first two terms ($K\theta$ and $B\dot{\theta}$) model the passive feedback torques due to
 96 ligament and muscle tone. On the contrary, $f_P(\theta_\Delta)$ and $f_D(\dot{\theta}_\Delta)$ model the
 97 active role played by the CNS that has been thought intermittent, depending
 98 on the portion of the phase plane the state is at a given time [10]. To be
 99 noted, the two terms depend respectively to the delayed sway angle and its
 100 time derivative. Indeed $\theta_\Delta = \theta(t - \Delta)$, where Δ represents the physiological
 101 neural delay that accounts for both the afferent and efferent neural information
 102 transmission [10]. The last term in the right hand side of (2) represents the
 103 internal postural noise, modeled as an additive Gaussian white noise $\xi(t)$ with
 104 standard deviation σ [10].

105 The switching policy adopted for the model was defined in [10] and used also
 106 in [6]. It can be summarized as follows:

$$\begin{cases} f_P(\theta_\Delta) = P\theta_\Delta; & f_D(\dot{\theta}_\Delta) = D\dot{\theta}_\Delta; & \text{if } \theta_\Delta(\dot{\theta}_\Delta - l\theta_\Delta) > 0 \\ f_P(\theta_\Delta) = 0; & f_D(\dot{\theta}_\Delta) = 0; & \text{otherwise} \end{cases} \quad (3)$$

107 where P and D represents the proportional and derivative gains of the active
 108 controller, while l characterizes the slope of the on-off boundary lines $\dot{\theta}_\Delta = l\theta_\Delta$
 109 [10, 7]. As highlighted in [7], for the closed loop system described above, the
 110 switching activity is driven by the portion of the phase plane where the active
 111 controller is turned on with respect to the whole phase plane (Fig. 1). This
 112 quantity can be defined as ρ and it is formally equivalent to [7]:

$$\rho = \frac{S_{on}}{S_{on} + S_{off}} \equiv 0.5 - \frac{\arctan(l)}{\pi} \quad (4)$$

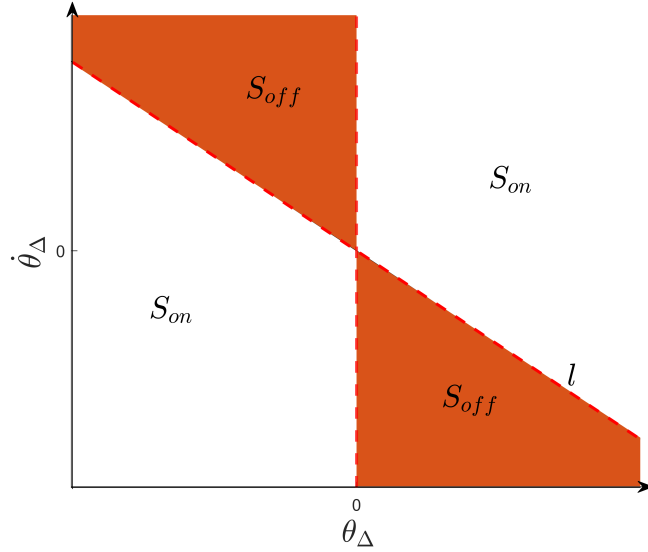


Figure 1: Schematic representation of the phase space portion in which the active controller is turned on (S_{on}) and off (S_{off}). The two regions were determined by the switching condition in equation (3) where l determines the on-off boundary region.

113 To be noted, if the active controller is continuously turned on, the S_{off} area is
 114 equal to zero ($\rho = 1$), and the model generalizes the continuous motor control
 115 paradigm [15, 7]. For a non-null S_{off} the active controller is turned on and off
 116 ($\rho < 1$) and the motor control paradigm is the intermittent one. Eventually,
 117 if the S_{on} area is zero ($\rho = 0$), the active controller never turns on and the
 118 pendulum stabilization can be reached only through the passive components of
 119 T .

120 However, as reported in [12], ankle stiffness alone cannot stabilize the upright
121 stance, and by following the line proposed in [10], the stiffness term K (see
122 equation (2)) was set at the 80% of mgh . In this way, an active control is
123 always required [7, 11]. To run the simulations, the model parameters and the
124 ICP, i.e. (P, D, ρ) , were set as reported in table 1. The forward Euler method
125 with a time step of 0.001 s was used to solve the delayed differential equation
126 given by (1) after substitution of T through (2). Further details regarding the
127 discretization and integration procedures can be found in [10, 7].

128 One thousand stable simulations of 60 s were run sampling (P, D, ρ) from
129 opportune uniform distributions (Table 1). For each simulation, the COP with
130 respect to the ankle joint was obtained following the relation [25]:

$$COP = COM - \frac{h}{g}C\ddot{O}M \quad (5)$$

131 where COM can be obtained by the sway data since is the projection of the cen-
132 ter of mass in the anterior posterior direction. More precisely, COM is obtained
as $COM = h \sin(\theta)$.

Table 1: Table shows the model parameters and the ICP used to simulate the model. P , D
and ρ were sampled from uniform distributions in plausible ranges [6, 7, 13]

m	I	h	B	K	g	Δ	σ	P	D	ρ
(kg)	(kg·m ²)	(m)	(N·m·s/rad)	(N·m/rad)	(m/s ²)	(s)	(N·m)	(N·m/rad)	(N·m·s/rad)	
60	60	1	4.0	471	9.81	0.2	0.2	$\mathcal{U}_{[294; 471]}$	$\mathcal{U}_{[0; 400]}$	$\mathcal{U}_{[0.3; 1]}$

133

134 2.2. Extended detrended fluctuation analysis

135 Given a time series $x(i)$ of length N , the DFA involves the transformation
136 of $x(i)$ in its profile $y(i)$ through an integration after mean removal [26, 24]:

$$y(k) = \sum_{i=1}^k [x(i) - \langle x \rangle], \quad \langle x \rangle = \frac{1}{N} \sum_{i=1}^N x(i) \quad (6)$$

137 The resulting profile or random walk undergoes to non-overlapping segmenta-
138 tions of equal length n . Then, for each segment of the profile, a local trend

139 $y_n(k)$ is computed through a linear fit in a least square sense [23]. When local
 140 trend is available, one can proceed by computing the fluctuation, or standard
 141 deviation of the signal profile around the local trend as:

$$F(n) = \sqrt{\frac{1}{N} \sum_{k=1}^N [y(k) - y_n(k)]^2} \quad (7)$$

142 The process is iterated for different segment size (n) in order to obtain $F(n)$
 143 over a possible large number of scales. In general, $F(n)$ presents a power law
 144 behavior of the type:

$$F(n) \sim n^\alpha \quad (8)$$

145 where the α -exponent can be estimated through the log-log representation of
 146 $F(n)$ versus n [24, 26].

147 What reported until now are the basic steps of the DFA. However, as high-
 148 lighted in [23], the inhomogeneity of the data, which can be due to multiple
 149 dynamics interactions, can lead to a consistent variability of the profile fluctu-
 150 ations around the local trend among the different signal epoch sizes (n). This
 151 can produce a departure from model (8), rendering more challenging the inter-
 152 pretation of the classical DFA. To mitigate this aspect, in [22, 23] the authors
 153 proposed a DFA extension, namely EDFA, that takes care of the heterogeneity
 154 in the RMS fluctuations. Hence, in addition to the canonical DFA, one can
 155 consider the following quantity:

$$dF(n) = \max[F_{loc}(n)] - \min[F_{loc}(n)] \quad (9)$$

156 where $dF(n)$ is the difference between the maximum and minimum local RMS
 157 fluctuations $F_{loc}(n)$ [23]. Here, the local RMS fluctuations of the signal profile
 158 $y(k)$ from the trend $y_n(k)$ depends on the epoch length (n). As observed in
 159 [23], also $dF(n)$ could change with n , following a power-law dependence with
 160 another scaling exponent β :

$$dF(n) \sim n^\beta \quad (10)$$

161 The EDFA was applied to each COP trace generated as described in section
 162 2.1, and both α and β were computed to evaluate how changes in the ICP

163 impact on the simulated COP time-series.

164 3. Results and Discussion

165 In Figure 2 the mean trends among all the simulated time series of both
166 F and dF are shown in the log-log scale. A greater variability is present at
167 higher time scales and an inverse relation exists between (n) and the frequency,
168 as underlined in [27]:

$$n(f) = \frac{f_s}{f} \quad (11)$$

169 where f_s is the sampling frequency and f is the considered frequency. This
170 suggests that modifications of the active controller parameters lead to changes
171 of balance response focused at the higher time scales and thus at the lower
172 frequency ranges [10], aligning with [28], where the effects of neural control on
173 COP data were observed in the lower bands (LB) frequency range of 0.5-0.1
174 Hz. Confirmations can be found also in [27], where part of such neural feedback
175 due to the visuo-vestibular information should be mirrored in COP time-series
176 at frequencies lower than 0.5 Hz [27]. This aspect supports the goodness of
177 the intermittent motor control paradigm, since modifications of its parameters
178 produce larger variations at the LB ranges (Fig. 3), thus in according with the
179 regulatory activity of the CNS in the human balance maintenance, focused on
180 the frequency LB [28, 10, 27]. For the above mentioned reasons, one can focus
181 on the fluctuations at the higher time scales to observe the behavior of both F
182 and dF in the LB.

183 The EDFA appears suitable for capturing variations in the active control
184 policy: observing the F and dF fluctuations restricted at the LB (Fig. 3), one
185 can appreciate that both type of fluctuations are affected by ICP variations and
186 dF showed a greater level of variability at all the (n) with respect to F , likely
187 indicating that dF responds to the same control parameters changes by greater
188 modifications of its value (Fig. 3).

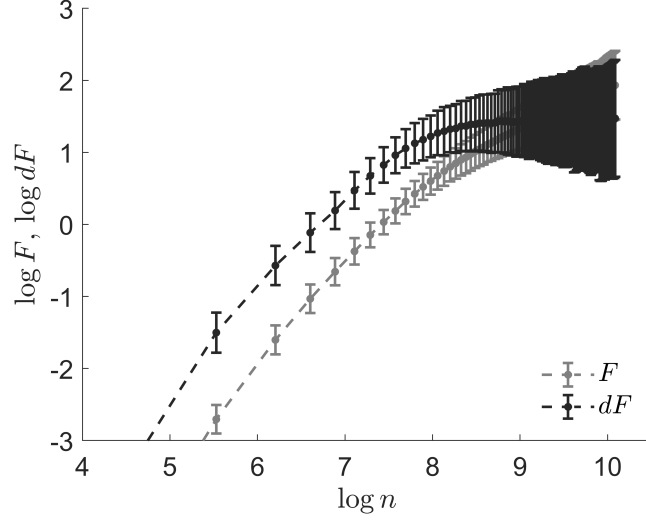


Figure 2: Log-log representation of the EDFA fluctuations in mean and standard deviation, the latter were computed over the 1000 synthetic COP time-series generated by the model.

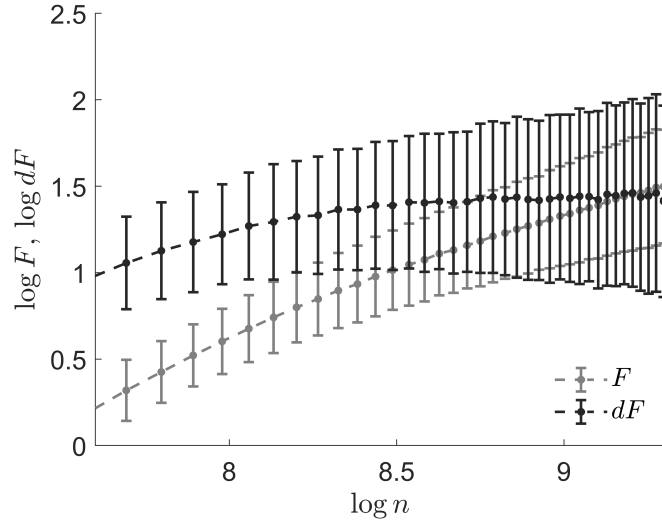


Figure 3: Log-log representation of the EDFA fluctuations in mean and standard deviation. Focus on the time scales that maps the frequency band 0.5-0.1 Hz.

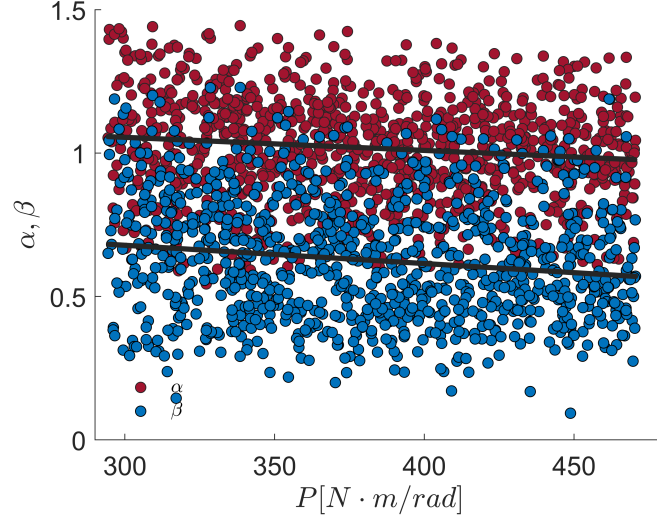


Figure 4: EDF coefficients α and β obtained for the simulated COP time series and scattered in relation to P parameter. The correlation coefficients results $r = -0.12$ and -0.15 , for α and β respectively. Figure shows also the linear trend between P and the coefficients.

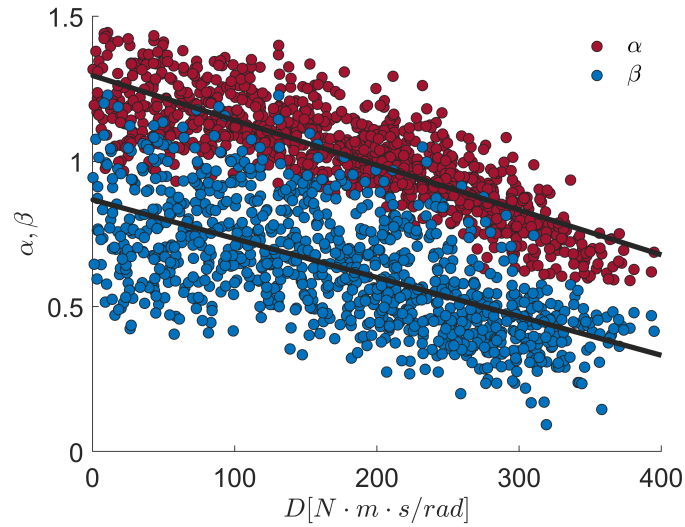


Figure 5: EDF coefficients α and β obtained for the simulated COP time series and scattered in relation to D parameter. The correlation coefficients results $r = -0.83$ and -0.63 , for α and β respectively. Figure shows also the linear trend between D and the coefficients.

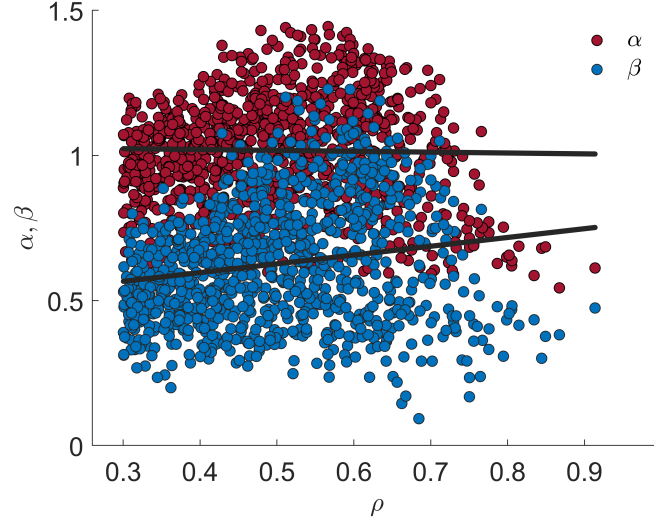


Figure 6: EDFA coefficients α and β obtained for the simulated COP time series and scattered in relation to ρ parameter. The correlation coefficients results $r = -0.019$ and 0.17 , for α and β respectively. Figure shows also the linear trend between ρ and the coefficients.

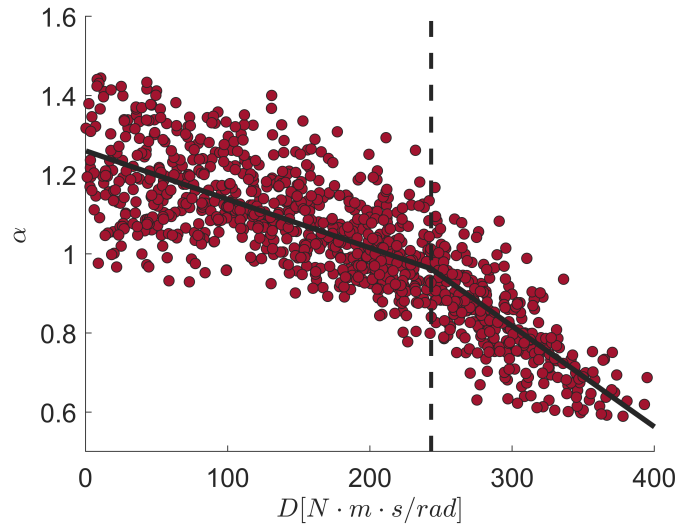


Figure 7: EDFA α coefficient scattered against D parameter. The two lines of the best fitting model are reported in black and the knot point is indicated with the dashed, vertical line.

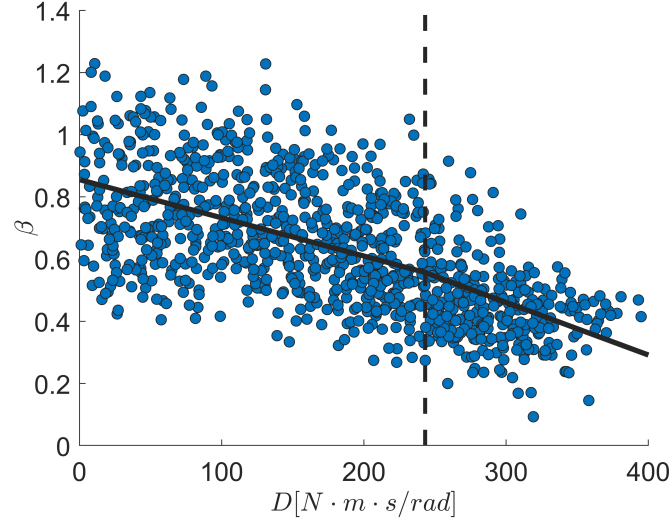


Figure 8: EDFA β coefficient scattered against D parameter. The two lines of the best fitting model are reported in black and the knot point is indicated with the dashed, vertical line.

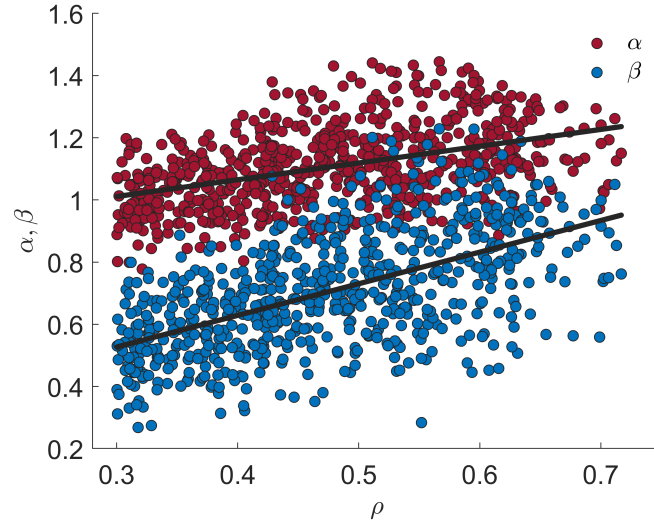


Figure 9: EDFA coefficients α and β obtained for the simulated COP time series and scattered in relation to ρ parameter for $D < 243 \text{ N} \cdot \text{m} \cdot \text{s} \cdot \text{rad}^{-1}$. Figure shows also the linear trend between ρ and the coefficients.

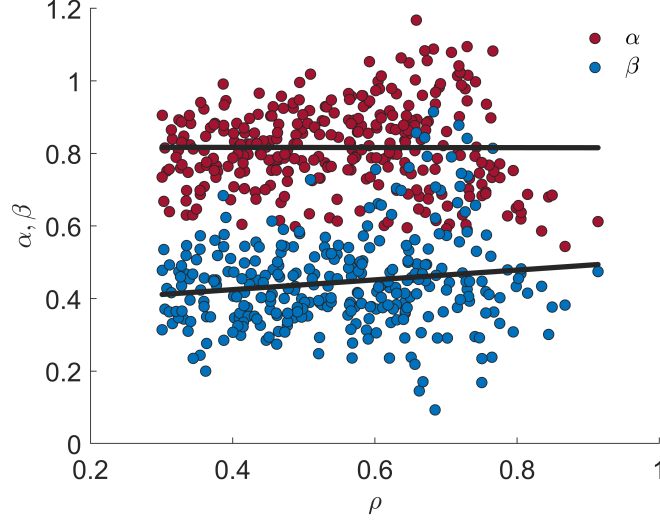


Figure 10: EDFA coefficients α and β obtained for the simulated COP time series and scattered in relation to ρ parameter for $D \geq 243 \text{ N} \cdot \text{m} \cdot \text{s} \cdot \text{rad}^{-1}$. Figure shows also the linear trend between ρ and the coefficients.

189 As highlighted in section 2.1, the motor control paradigm examined in this
190 study depends upon ρ , P , and D . The EDFA coefficients showed different
191 relationship with the above mentioned parameters when considered over their
192 whole range of variation (Table 1). Globally, the P parameter did not appear
193 related to neither the long term correlation properties, nor to the inhomogeneity
194 of the simulated COP time-series, as showed by the poor correlation between
195 P , α , and β (Fig. 4). This confirms that when P is large enough to compensate
196 the portion of the gravitational toppling torque not counteracted by the passive
197 muscles properties (K and B), a wide range of values is admissible for P and
198 thus, with respect to D , its role becomes less crucial for the control model [6, 10].
199 The latter aspect aligns with the strong relation observed between both EDFA
200 coefficients and D (Fig. 5), highlighted by the significant correlations of the
201 derivative gain with α and β ($r = -0.83$ and $r = -0.63$, $p < 0.0001$). In passing,
202 the $\alpha - D$ relation (Fig. 5) points out that the higher is D , the lower is the
203 long-term correlation of the COP timeseries, in agreement with previous studies

204 that reported lower values of α in elderly populations, where a degraded motor
205 control can be assumed [19, 29]. This was confirmed also in [7], where it was
206 observed that patients affected by Parkinson’s disease showed higher D values
207 if compared to healthy elderly. Indeed, control schemes with large derivative
208 gain constitutes an energetically inefficient control strategy, with inflexible and
209 non-reactive stabilizing mechanism, marked by lower α values [7].

210 As happened for P , also ρ did not show any significant correlation with α
211 and β coefficients (Fig. 6), indicating that, despite the significant role of ρ
212 in defining the exchange between the ON and OFF sub-dynamics (see section
213 2.1), it appears to be not directly related with the stochastic properties of COP
214 timeseries quantified through the EDFA. In addition, it deserves to be noted
215 that, within the range of P and D values selected in this study (Table 1), stable
216 simulations were obtained for ρ up to $\simeq 0.9$, although ρ was free to vary with
217 the upper bound set to 1 (Table 1). This indicates that the condition for a fully
218 continuous control ($\rho = 1$) was not reached and thus findings of this study hold
219 when an intermittent control takes place.

220 For what concerns the β coefficient, it can be observed that the inhomogene-
221 ity of the COP timeseries decreases for progressively higher values of D (Fig. 5).
222 The coefficient β was defined to indicate departure from the power law behavior
223 (8), since the standard deviation of the profile from the local trend (7) can vary
224 significantly among the different segments [22]. A reduction of inhomogeneity
225 implies COP timeseries characterized by regular oscillatory fluctuations, closer
226 to a stationary behavior. Hence, the β coefficient can provide additive informa-
227 tion regarding the organization of biological signals in terms of complexity, since
228 it provides a quantitative measure of local transients [22]. The lower β values
229 observed for increasing derivative gains appears in agreement also with the *loss*
230 *of complexity* paradigm [30]. This hypothesis essentially states that healthy
231 physiological systems produce responses that are complex in the sense of non
232 linear correlations and long-term dynamics, while a functions’ breakdown, due
233 to aging or disease, leads to less complex outputs that mirror a reduced ability
234 in producing an adaptive set of responses when facing motor, cognitive or neu-

235 rological needs [31, 32]. Thus, the reduction of β coefficient highlights a loss of
 236 fine-structures in COP epochs and it suggests a reduced capability to cope with
 237 balance demands, relying on a set of few and repeatable postural patterns with
 238 a limited physiological adaptability. Hence, a lower degree of inhomogeneity
 239 could reflect a rearrangement in the CNS motor control schemes due to certain
 240 pathologies, resembling an inefficient tuning of the IP active controller [7, 33].

241 The above mentioned analysis indicates that, among the three ICP, D gain
 242 alone reflects changes in the long-term correlation and inhomogeneity properties
 243 of the whole COP timeseries. This aspect is strengthened also by considering
 244 separately $\alpha - D$ and $\beta - D$ relations (Figs. 7 and 8). In both cases, it appeared
 245 that the inter-dependence between D and EDFA coefficients can be fitted with
 246 two straight lines characterized by different slopes, highlighting the possible
 247 existence of two different relationships, depending upon D values. In order to
 248 test this hypothesis, both the $\alpha - D$ and $\beta - D$ were fitted through a least-
 249 square spline approach [34], testing respectively the existence of three models,
 250 described by one, two, and three polynomials of order 1. The criterion used
 251 for assessing the best model was the normalized Akaike's information criterion
 252 (nAIC) [35], for which the most accurate model presents the lowest nAIC. For
 253 both $\alpha - D$ and $\beta - D$ data distributions, the best fitting model was that with a
 254 single knot point and thus with two lines: in this case the nAIC resulted equal
 255 to -4.67 versus -4.57 (one line) and -4.40 (three lines) for $\alpha - D$. Similarly,
 256 for $\beta - D$ the two-lines model presented a nAIC of -3.67 versus -3.60 (one line)
 257 and -3.52 (three lines). In addition, in both cases the crossing point between
 258 the two lines (the knot), presented the same value, i.e. $D = 243 \text{ N} \cdot \text{m} \cdot \text{s} \cdot \text{rad}^{-1}$
 259 (Figs. 7 and 8).

260 Given the presence of two different kind of relations between D and EDFA
 261 coefficients, a further analysis was performed regarding the correlation between
 262 α and β with the other two control parameters, i.e. P and ρ . Hence, those P and
 263 ρ values for which the correspondent D gain was respectively $< 243 \text{ N} \cdot \text{m} \cdot \text{s} \cdot \text{rad}^{-1}$
 264 and $\geq 243 \text{ N} \cdot \text{m} \cdot \text{s} \cdot \text{rad}^{-1}$ were separately taken into account. To be noted, such D
 265 value was obtained directly from the above mentioned data-driven analysis and

thus it cannot be claimed that it represents a critical value for the intermittent control scheme. Its possible physical meaning, however, deserves to be carefully investigated in future studies, also in relation to the other ICP.

Regarding the proportional gain, as happened when the $\alpha - P$ and $\beta - P$ correlations were examined over the entire range of the proportional gain (Fig. 4), neither α nor β showed any direct relation with P ($r = -0.36$ and -0.32 for $D < 243 N \cdot m \cdot s \cdot rad^{-1}$ and $r = -0.19$ and -0.11 for $D \geq 243 N \cdot m \cdot s \cdot rad^{-1}$). This supports once more that within the range of values assumed by P in this study, its variations seem to not consistently affect the COP fractal properties measured by EDFA.

On the other hand, the ρ parameter showed a different behavior with respect to α and β depending upon the values assumed by the derivative gain. When D is lower than $243 N \cdot m \cdot s \cdot rad^{-1}$, both α and β showed a significant ($p < 0.0001$) correlation with ρ ($r = 0.44$ and 0.61 , respectively, Fig. 9). This suggests that the stochastic behavior and the inhomogeneity of a timeseries, quantified by the EDFA coefficients, manifest a direct relationship with the intermittent nature of balance control when D assumes typical values for this control strategy [7]. Incidentally, this is also in agreement with ρ values that not overcome $\simeq 0.7$, which permits to exploit the two main features of the intermittent control: the stable manifold belonging to the OFF-dynamics and the spiraling state steering induced by the delayed unstable dynamic of the ON-subsystem. This eventually permits to obtain limit cycle stability without the need of greater control efforts [7]. In addition, the correlation between α and two control parameters (D and ρ) aligns with the findings by Yamamoto et al. [28], who reported that the slope of the COP power spectrum at the LB, which is directly related to α [36], is a universal characteristic of postural sway, associated to neural control strategies. Considering that, despite both trends are significant, β highlights a greater capability in detecting changes in ρ , if compared to α , and thus it further supports the use of the extended version of the DFA for analyzing posturographic data.

Finally, it is interesting to note that the α coefficient maintains in any case values quite close to 1 (Fig. 9), possibly referring to an attempt to maintain

the output of the balance regularization, i.e. the COP, close to a $1/f$ process. Indeed, the latter is frequently encountered in different physiological time-series, characterizing a healthy motor control [27, 37, 38]. On the other hand, the β coefficient covered a larger set of values (Fig. 9), pointing out that the simulated COP timeseries exhibited different degrees of irregularity in their local structures [23, 22]. The latter can be associated with the complexity of the physiological system generating the data [22], which in healthy conditions is commonly characterized by a higher complexity [38, 39], leading in turn to an enhanced robustness and adaptability of the response [39, 40].

Present results indicate that, when relatively low D values are used in the active controller, the ρ parameter is connected to the degree of inhomogeneity of the COP and thus to the complexity of the balance regulation. This can motivate additional studies aimed at investigating how the tuning of the S_{on} and S_{off} regions impacts on the irregularity and complexity of the COP fluctuations. It should be noted that the EDFA investigated in this study provides a single-scale analysis, accounting for a global description of the data [23, 22], whereas many previous studies demonstrated the value of a multi-scale approach for COP timeseries [14, 19, 27, 32, 40]. This is also supported by present results, which highlighted different dynamics over different temporal scales (Fig. 2). Therefore, future works should be devoted to apply EDFA in a multi-scale analysis, in order to gain insights regarding the inhomogeneity of COP timeseries over different sub-dynamics.

When the derivative gain assumes values higher than $243 \text{ N} \cdot \text{m} \cdot \text{s} \cdot \text{rad}^{-1}$, the P gain remains unrelated to both α and β , as highlighted by the poor correlation coefficients ($r = -0.19$ and -0.11 , respectively). In this case the same holds also for the ρ parameter (Fig. 10), for which the correlations observed in the previous case completely disappeared ($r = -0.0021$ for $\alpha - \rho$ and $r = -0.14$ for $\beta - \rho$). A possible explanation for this behavior can be proposed considering that, for such range of D values, the S_{on} dynamics can stabilize the IP process *per se* [7], without the need for switching between sub-dynamics, since with this range of D values ($\geq 243 \text{ N} \cdot \text{m} \cdot \text{s} \cdot \text{rad}^{-1}$) the (P, D) of the ON-subsystem is

located inside the stability region reported by Suzuki et al. [7]. In this context, the control policy mimics a stabilizing delayed continuous control [7] and thus it is reasonable to assume that ρ becomes less crucial within this control scheme, loosing its relations with EDFA coefficients.

Outcomes of this study indicate that the α and β coefficients introduced by the EDFA provides additional information on local COP structures, which in turns are related to the parameters of the intermittent control model. Further, EDFA resulted able to highlight subtle properties of sway fluctuation data which can be observed if different ranges of control parameters' values are separately taken into account. Hence, EDFA can be used together with the classical DFA exponent to better characterize the upright balance maintenance under the intermittent control regime, since inhomogeneity and long term correlations can be useful descriptors of the hidden postural control paradigm.

4. Conclusion

In this study, the EDFA was used to investigate the COP time-series generated by using an IP model, intermittently controlled at the ankle. The IP model was used to simulate the dynamics of the human balance maintenance in the anterior-posterior direction [10]. The intermittent motor control paradigm confirmed to be adequate to simulate COP that presented characteristics of long-term correlation, as those observed for real data [4]. Moreover, the concept of inhomogeneity introduced in the EDFA turned out to be suitable for characterizing inner properties of the balance regulation output. The β coefficient was coupled to the hidden controller parameter D and ρ , showing different relations depending upon the derivative gain values investigated.

In addition, the modeling approach here employed resulted useful to highlight possible interpretation that the EDFA analysis can provide when applied to real data. Indeed, in a real scenario, functional rearrangements of the CNS can be identified in changes in the controller parameters, using opportune identification procedures [33, 7]. Hence, EDFA, embedding the concept of inhomogeneity

geneity, can be particularly suitable in posturography to highlight differences in balance strategies between healthy and pathological groups. Lastly, the choice of using COP rather than other time series, i.e., COM and joints angles, lies on an important practical consideration, since COP is directly measurable from force-plate and it does not require any patient instrumentation or estimation procedure.

References

- [1] V. Lippi, Prediction in the context of a human-inspired posture control model, *Robotics and Autonomous Systems* 107 (2018) 63–70.
- [2] T. Mergner, K. Tahboub, Neurorobotics approaches to human and humanoid sensorimotor control., *Journal of physiology, Paris* 103 (3-5) (2009) 115–118.
- [3] J. Błaszczyk, R. Orawiec, D. Duda-Kłodowska, G. Opala, Assessment of postural instability in patients with parkinson’s disease, *Experimental Brain Research* 183 (1) (2007) 107–114.
- [4] H. Amoud, M. Abadi, D. J. Hewson, V. Michel-Pellegrino, M. Doussot, J. Duchêne, Fractal time series analysis of postural stability in elderly and control subjects, *Journal of neuroengineering and rehabilitation* 4 (1) (2007) 12.
- [5] A. Bottaro, Y. Yasutake, T. Nomura, M. Casadio, P. Morasso, Bounded stability of the quiet standing posture: an intermittent control model, *Human movement science* 27 (3) (2008) 473–495.
- [6] P. Morasso, A. Cherif, J. Zenzeri, Quiet standing: The single inverted pendulum model is not so bad after all, *PloS one* 14 (3) (2019) e0213870.
- [7] Y. Suzuki, A. Nakamura, M. Milosevic, K. Nomura, T. Tanahashi, T. Endo, S. Sakoda, P. Morasso, T. Nomura, Postural instability via a loss of intermittent control in elderly and patients with parkinson’s disease: A model-

- 384 based and data-driven approach, *Chaos: An Interdisciplinary Journal of*
385 *Nonlinear Science* 30 (11) (2020) 113140.
- 386 [8] I. Schut, J. Pasma, J. Roelofs, V. Weerdesteyn, H. van der Kooij,
387 A. Schouten, Estimating ankle torque and dynamics of the stabilizing mech-
388 anism: no need for horizontal ground reaction forces, *Journal of Biomechan-*
389 *ics* (2020) 109813.
- 390 [9] R. J. Peterka, Sensory integration for human balance control, *Handbook of*
391 *clinical neurology* 159 (2018) 27–42.
- 392 [10] Y. Asai, Y. Tasaka, K. Nomura, T. Nomura, M. Casadio, P. Morasso, A
393 model of postural control in quiet standing: robust compensation of delay-
394 induced instability using intermittent activation of feedback control, *PLoS*
395 *One* 4 (7) (2009) e6169.
- 396 [11] P. G. Morasso, M. Schieppati, Can muscle stiffness alone stabilize upright
397 standing?, *Journal of Neurophysiology* 82 (3) (1999) 1622–1626.
- 398 [12] P. G. Morasso, V. Sanguineti, Ankle muscle stiffness alone cannot stabilize
399 balance during quiet standing, *Journal of neurophysiology* 88 (4) (2002)
400 2157–2162.
- 401 [13] Y. Suzuki, T. Nomura, M. Casadio, P. Morasso, Intermittent control with
402 ankle, hip, and mixed strategies during quiet standing: a theoretical pro-
403 posal based on a double inverted pendulum model, *Journal of Theoretical*
404 *Biology* 310 (2012) 55–79.
- 405 [14] J. J. Collins, C. J. De Luca, Open-loop and closed-loop control of posture: a
406 random-walk analysis of center-of-pressure trajectories, *Experimental brain*
407 *research* 95 (2) (1993) 308–318.
- 408 [15] R. J. Peterka, Postural control model interpretation of stabilogram diffusion
409 analysis, *Biological cybernetics* 82 (4) (2000) 335–343.

- [16] L. Baratto, P. G. Morasso, C. Re, G. Spada, A new look at posturographic analysis in the clinical context: sway-density versus other parameterization techniques, *Motor control* 6 (3) (2002) 246–270.
- [17] P. Morasso, Centre of pressure versus centre of mass stabilization strategies: the tightrope balancing case, *Royal Society open science* 7 (9) (2020) 200111.
- [18] T. E. Prieto, J. B. Myklebust, R. G. Hoffmann, E. G. Lovett, B. M. Myklebust, Measures of postural steadiness: differences between healthy young and elderly adults, *IEEE Transactions on biomedical engineering* 43 (9) (1996) 956–966.
- [19] J. Collins, C. De Luca, A. Burrows, L. Lipsitz, Age-related changes in open-loop and closed-loop postural control mechanisms, *Experimental Brain Research* 104 (3) (1995) 480–492.
- [20] V. M. Zatsiorsky, M. Duarte, Rambling and trembling in quiet standing, *Motor control* 4 (2) (2000) 185–200.
- [21] M. Jacono, M. Casadio, P. G. Morasso, V. Sanguineti, The sway-density curve and the underlying postural stabilization process, *Motor control* 8 (3) (2004) 292–311.
- [22] A. N. Pavlov, A. S. Abdurashitov, A. Koronovskii Jr, O. N. Pavlova, O. Semyachkina-Glushkovskaya, J. Kurths, Detrended fluctuation analysis of cerebrovascular responses to abrupt changes in peripheral arterial pressure in rats, *Communications in Nonlinear Science and Numerical Simulation* 85 (2020) 105232.
- [23] A. Pavlov, A. Dubrovsky, A. Koronovskii Jr, O. Pavlova, O. Semyachkina-Glushkovskaya, J. Kurths, Extended detrended fluctuation analysis of electroencephalograms signals during sleep and the opening of the blood–brain barrier, *Chaos: An Interdisciplinary Journal of Nonlinear Science* 30 (7) (2020) 073138.

- 438 [24] O. Pavlova, A. Pavlov, Scaling features of intermittent dynamics: Differ-
439 ences of characterizing correlated and anti-correlated data sets, *Physica A:
440 Statistical Mechanics and its Applications* 536 (2019) 122586.
- 441 [25] D. A. Winter, *Biomechanics and motor control of human gait: normal,
442 elderly and pathological*, 1991.
- 443 [26] C.-K. Peng, S. Havlin, H. E. Stanley, A. L. Goldberger, Quantification
444 of scaling exponents and crossover phenomena in nonstationary heartbeat
445 time series, *Chaos: an interdisciplinary journal of nonlinear science* 5 (1)
446 (1995) 82–87.
- 447 [27] P. Gilfriche, V. Deschodt-Arsac, E. Blons, L. M. Arsac, Frequency-specific
448 fractal analysis of postural control accounts for control strategies, *Frontiers
449 in physiology* 9 (2018) 293.
- 450 [28] T. Yamamoto, C. E. Smith, Y. Suzuki, K. Kiyono, T. Tanahashi, S. Sakoda,
451 P. Morasso, T. Nomura, Universal and individual characteristics of postural
452 sway during quiet standing in healthy young adults, *Physiological reports*
453 3 (3) (2015) e12329.
- 454 [29] A. Tigrini, F. Verdini, S. Fioretti, A. Mengarelli, Center of pressure plausi-
455 bility for the double-link human stance model under the intermittent con-
456 trol paradigm, *Journal of Biomechanics* 128 (2021) 110725.
- 457 [30] L. A. Lipsitz, Dynamics of stability: the physiologic basis of functional
458 health and frailty, *The Journals of Gerontology Series A: Biological Sciences
459 and Medical Sciences* 57 (3) (2002) B115–B125.
- 460 [31] A. L. Goldberger, C.-K. Peng, L. A. Lipsitz, What is physiologic complexity
461 and how does it change with aging and disease?, *Neurobiology of Aging*
462 23 (1) (2002) 23–26.
- 463 [32] M. Costa, A. Priplata, L. Lipsitz, Z. Wu, N. Huang, A. L. Goldberger,
464 C.-K. Peng, Noise and poise: enhancement of postural complexity in the

465 elderly with a stochastic-resonance-based therapy, EPL (Europhysics Let-
466 ters) 77 (6) (2007) 68008.

467 [33] M. L. Corradini, S. Fioretti, T. Leo, R. Piperno, Early recognition of postu-
468 ral disorders in multiple sclerosis through movement analysis: a modeling
469 study, IEEE Transactions on Biomedical Engineering 44 (11) (1997) 1029–
470 1038.

471 [34] X. Zhang, J. G. Andrews, Downlink cellular network analysis with multi-
472 slope path loss models, IEEE Transactions on Communications 63 (5)
473 (2015) 1881–1894.

474 [35] L. Ljung, System identification-theory for the user 2nd edition ptr prentice-
475 hall, 1999.

476 [36] T. Nomura, S. Oshikawa, Y. Suzuki, K. Kiyono, P. Morasso, Modeling
477 human postural sway using an intermittent control and hemodynamic per-
478 turbations, Mathematical Biosciences 245 (1) (2013) 86–95.

479 [37] C. Fu, Y. Suzuki, P. Morasso, T. Nomura, Phase resetting and intermittent
480 control at the edge of stability in a simple biped model generates 1/f-like
481 gait cycle variability, Biological cybernetics 114 (1) (2020) 95–111.

482 [38] J. M. Hausdorff, Gait dynamics in parkinson’s disease: common and dis-
483 tinct behavior among stride length, gait variability, and fractal-like scaling,
484 Chaos: An Interdisciplinary Journal of Nonlinear Science 19 (2) (2009)
485 026113.

486 [39] S. Thurner, C. Mittermaier, K. Ehrenberger, Change of complexity patterns
487 in human posture during aging, Audiology and Neurotology 7 (4) (2002)
488 240–248.

489 [40] B. Manor, M. D. Costa, K. Hu, E. Newton, O. Starobinets, H. G. Kang,
490 C. Peng, V. Novak, L. A. Lipsitz, Physiological complexity and system
491 adaptability: evidence from postural control dynamics of older adults, Jour-
492 nal of Applied Physiology 109 (6) (2010) 1786–1791.